

Concerted Effects of Substituents in the Reaction of •OH Radicals with Aromatics: The Cresols

Guadalupe Albarran[†] and Robert H. Schuler^{*‡}

Instituto de Ciencias Nucleares, UNAM, Circuito Exterior C.U., 04510 Mexico, D.F., and Radiation Laboratory, University of Notre Dame, Notre Dame, Indiana 46556

Received: July 19, 2005; In Final Form: August 17, 2005

The concerted effects of hydroxyl and methyl substituents in controlling the site of •OH radical attack on aromatics in aqueous solutions are explored using the cresols as typical examples. The distributions of dihydroxytoluenes produced in the radiolysis of aqueous solutions of the cresols containing ferricyanide as a radical oxidant were examined by capillary electrophoretic and liquid chromatographic methods. Because •OH is a strong electrophile, it adds preferentially at the electron-rich sites of an aromatic ring. As a result, the observed distributions of dihydroxytoluenes reflect the charge distributions in the cresols. It is shown that in the case of *m*-cresol the hydroxyl substituent has a dominant *ortho*–*para* directing effect similar to that observed for phenol. In *o*- and *p*-cresol, this effect is modified, indicating that the methyl substituent has a significant effect on the electronic structure of those cresols. Correlation of the charge distribution in the cresols indicated by the observed distribution of dihydroxytoluenes with the unpaired spin distribution in the corresponding methylphenoxy radicals demonstrates that the electronic structures of *o*- and *p*-cresol and their corresponding phenoxy radicals are similarly affected by hydroxyl and methyl substitution. Addition of •OH at the methyl-substituted positions of *o*- and *p*-cresol to produce *o*- and *p*-dienone is also reported. The observation of these dienones demonstrates that addition of •OH at the *ipso* positions of alkylated aromatics can be of considerable importance. Mass spectrometric studies show that these dienones have relatively higher proton affinities than their isomeric analogues.

I. Introduction

Addition of •OH radical to most aromatics is essentially diffusion controlled,¹ producing hydroxycyclohexadienyl radicals that can be oxidized to the corresponding phenols by organic oxidants such as quinones² and various inorganic oxidants.^{3,4} Provided that the redox potential of the oxidant used is sufficiently high, the relative yields of the phenolic products produced provide information on the position of attack of •OH radical on the aromatic. While the oxidizing power of quinones may not be sufficient to oxidize all cyclohexadienyl radicals,² it has been shown previously that in the radiolysis of aqueous solutions of benzene millimolar concentrations of ferricyanide are sufficient to oxidize the intermediate hydroxycyclohexadienyl radicals to phenol quantitatively.⁴ In the present study, ferricyanide is similarly used to oxidize the methylhydroxycyclohexadienyl radicals initially resulting from •OH addition to the cresols to produce the corresponding dihydroxytoluenes.

Because •OH is a strong electrophile, it probes the charge distribution in its attack on aromatics. In the case of phenol, the distribution of dihydroxybenzenes observed demonstrates that addition occurs preferentially at the electron-rich sites *para* and *ortho* to the OH substituent.^{2,5,6} The distribution of hydroxylated toluenes produced in its reaction with toluene shows that the methyl substituent has a similar, but considerably less, directing effect than does OH.⁷ The present study examines the reaction of •OH with the cresols to provide information on

the concerted effects of hydroxyl and methyl substituents in controlling the site of •OH addition. It is shown here that presence of the methyl substituent modifies the directing effect of the OH substituent and that the combined effects of the two substituents on the charge distribution in the cresols are similar to their effects on the unpaired spin distributions in the corresponding methylphenoxy radicals.

As in the case of *p*-cresol, where it has been shown that 4-hydroxy-4-methyl-2,5-cyclohexadiene-1-one (subsequently referred to as *p*-dienone) results from addition to its ring at its methyl position,⁸ the present study shows that 2-hydroxy-2-methyl-3,5-cyclohexadiene-1-one (subsequently referred to as *o*-dienone) similarly results from •OH addition at the methyl position of *o*-cresol. These findings emphasize that •OH addition at *ipso* positions of alkylated aromatics can be of considerable importance.

The details of this study follow.

II. Experimental Section

Aqueous solutions 5 mM in *p*-cresol, *m*-cresol, or *o*-cresol, saturated with N₂O and containing 2.5 mM K₃Fe(CN)₆, were irradiated in a ⁶⁰Co source at a dose rate of 2.2 kGy/h (2.3 × 10¹⁷ eV/g/min).⁹ Solutions were at their natural pH. At this dose rate, •OH is produced in N₂O-saturated solutions at a rate of 28 μM/min. The N₂O served to convert the hydrated electrons produced in water radiolysis to •OH, and the ferricyanide served to oxidize the methylhydroxycyclohexadienyl radicals that initially result from •OH addition. Analyses were carried out immediately after irradiation.

The radiolytic products were examined by high pressure liquid chromatography (HPLC) using a Waters Millennium system

* To whom correspondence should be addressed. E-mail: schuler.1@nd.edu.

[†] Instituto de Ciencias Nucleares, UNAM.

[‡] University of Notre Dame.

with a 996 diode array detector. Spectra were recorded spectrophotometrically from 200 to 400 nm in 3-D format. Analyses were at room temperature using gradient elution methods. Separations were on a 5 μ Phenomenex Luna C-8 column (250 mm \times 4.6 mm) at a flow rate of 0.5 cm³/min. Initially, the eluent was water containing 10% methanol and 0.027 M formic acid. This elution was isocratic for 15 min, followed by increases of methanol to 50% at 40 min. Chromatograms were extracted from these recordings at appropriate wavelengths and spectra at the chromatographic maxima. Proper identification of the hydroxybenzyl alcohol, dihydroxytoluene, and methylquinone peaks was assured by comparison of retention times and spectra with authentic samples. The spectra of the dihydroxytoluenes are similar but sufficiently different as to provide positive identification. Additional products observed include *o*- and *p*-dienone (see below) and a variety of secondary products. The dienones were identified from their spectra and mass patterns as discussed below.

Concentrations of the radiolytic products were determined from peak areas obtained using the routines in the Millennium software. All of the dihydroxytoluenes have modestly intense bands with similar sensitivities in the 220 nm region and weaker bands in the 275 nm region. Except for *o*-dienone, the chromatographic sensitivities were determined using reference samples chromatographed under similar conditions. The sensitivity of *o*-dienone was estimated by comparison of its 125 mass peak with that of *p*-dienone (see below).

The irradiated samples were also examined with an Agilent 1100 LC/MS system that provided spectrophotometric and mass spectrometric information on the radiolytic products. The sample passed through the spectrophotometric detector first with a \sim 0.1 min delay in the mass recordings. Separations were carried out isocratically on a 50 mm \times 4.6 mm i.d. Alltech Alltima 3 μ C-18 column using 10% methanol containing 0.17 M acetic acid as the eluent. In the mass spectrometric studies, atmospheric pressure chemical ionization (CI) and electrospray (ES) ion sources were used, and both positive and negative chromatograms were recorded in the total ion (SCAN) mode and at selected masses in the single ion detection (SIM) mode. The SCAN recordings allowed mass spectra of the individual peaks and chromatograms at specific masses to be displayed. In the positive ion ES recordings, the dihydroxytoluenes exhibited significant peaks at mass 125 and the benzyl alcohols at mass 107. Methylquinone concentrations could not be determined accurately from these electrospray recordings since methylquinone exhibits only weak peaks at masses 123 and 125. Because the secondary products do not contribute at these masses, these ES recordings discriminate against contributions from secondary products. The CI recordings were of lower intensity and, as described in a following section, more complex. The negative ion recordings provided very little information other than that available from the positive ion recordings. Where reference samples were available to establish sensitivities, concentrations of the products were determined from the areas of these mass chromatographic peaks.

These HPLC studies were complemented by capillary electrophoretic (CE) analyses. A Hewlett-Packard G1600^{3D} capillary electrophoretic system, equipped with a diode array detector and a high sensitivity detection cell having an optical path length of 1.2 mm, was used. Because the peak widths were considerably less than those in the HPLC studies, the sensitivities of these two approaches were similar. Electrophoretic data were also recorded in 3-D format. Separations were with a 72 cm \times 75 μ m capillary at an applied voltage of +30 kV. To separate

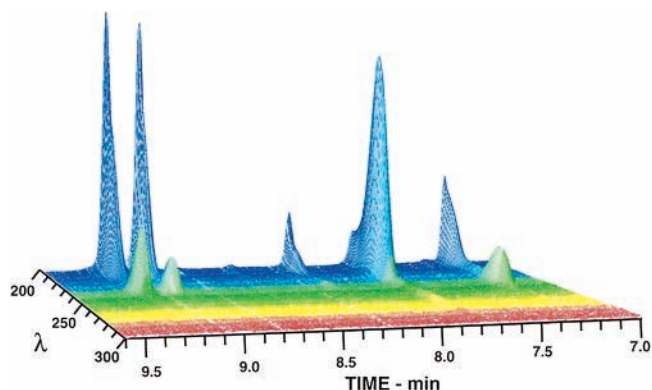


Figure 1. Three-dimensional display of the electrophoretic data for a N₂O saturated aqueous solution 5 mM in *m*-cresol and 2.5 mM in ferricyanide irradiated to a dose of 2.2 kGy. The peaks are identified in the caption to Figure 2. See Figure 1S for a contour plot of these data.

the analytes that were mostly neutral phenolics in most studies, the electrophoretic buffer contained 50 mM sodium dodecyl sulfate (SDS). The analytical approach used here is, therefore, more properly described as micellar electrokinetic capillary chromatography (MECC). Because the electrophoresis was controlled by electro-osmotic flow, anion migration was to the negative terminal. The buffer was usually 10 mM phosphate at pH 7. Borate (20 mM) at pH 9.3 was used in selected cases. The capillary was flushed with the buffer solution before each injection so that analyses could be carried out considerably more rapidly and conveniently than with HPLC. As in the HPLC studies, peaks were identified from spectra extracted from the 3-D data and concentrations determined from peak areas in electropherograms extracted at appropriate wavelengths. Peak areas were determined using routines in the HP software or, alternatively, because most peaks were essentially Gaussian in shape, using the Gaussian routines in *ORIGIN*.¹⁰

III. Results: LC and CE Studies

A. *m*-Cresol. *m*-Cresol represents the simplest of the three examples in that the products initially produced in significant yield result solely from addition of \bullet OH at its four unsubstituted positions. Figure 1 is a 3-D plot of electrophoretic data for an aqueous solution 5 mM in *m*-cresol irradiated to a dose of 2.2 kGy. A contour plot of the data of Figure 1 is given in the Supporting Information as Figure 1S. These plots are typical of the CE data obtained in these studies.

In Figures 1 and 1S, one sees contributions of the four expected dihydroxytoluenes (methylhydroquinone, 5-methylresorcinol, 3-methylcatechol, and 4-methylcatechol) at, respectively, 7.23, 8.23, 9.03, and 9.23 min. Because of the low yield of 5-methylresorcinol, only its absorption below 230 nm contributes in Figure 1S. In addition, the peak at 7.81 min is readily identified as methylquinone because of its intense 250 nm absorption. This quinone results from partial oxidation of methylhydroquinone prior to analysis.

While 3-hydroxybenzyl alcohol might also be expected to result from hydroxylation of the methyl group, reference electrophoretic data show that it migrates just before methylquinone. It is not apparent in Figure 1 or in related contour plots, but it is observed as a weak peak in MS chromatograms that indicates its yield to be only \sim 0.01 (see below). There is no indication of any product that might result from addition to the ring at the methyl position. With prolonged irradiation, secondary products appear in low concentration.

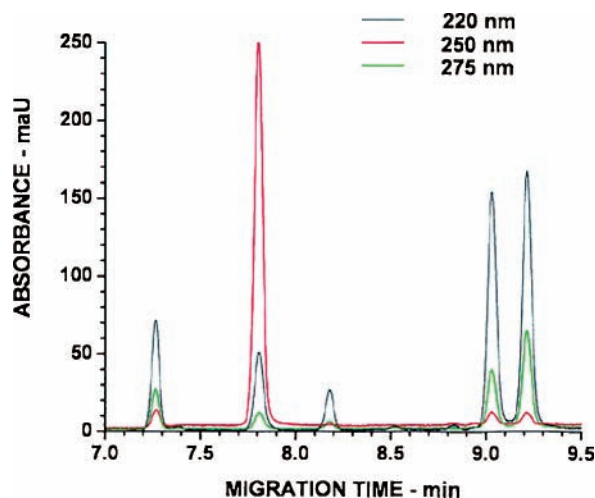


Figure 2. Electropherograms extracted from Figure 1 at 220, 250, and 275 nm. Peaks at 7.23, 7.81, 8.18, 9.03, and 9.23 min are identified, respectively, as methylhydroquinone, methylquinone, 5-methylresorcinol, 3-methylcatechol, and 4-methylcatechol.

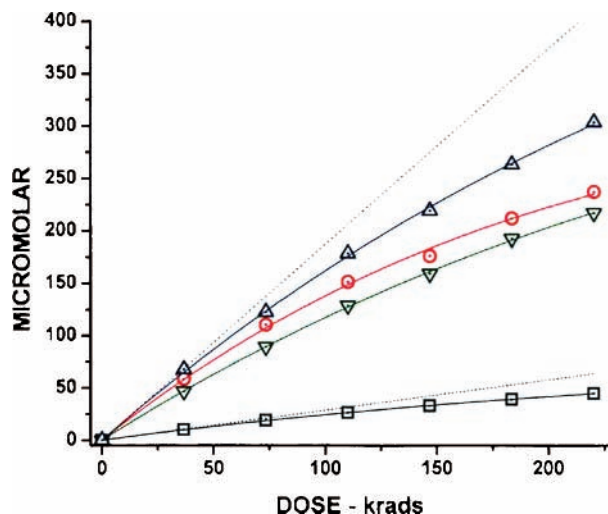


Figure 3. Dependence of product concentration on dose: sum of quinone and hydroquinone (blue); 4-methylcatechol (red); 3-methylcatechol (green); 5-methylresorcinol (black). Data are fitted by eq 1 given in the text. Dotted lines represent tangents to the fitted data at zero dose.

Electropherograms extracted from the data of Figure 1 are given in Figure 2. One notes that the peaks are Gaussian-shaped and that 3-methylcatechol and 4-methylcatechol are well-resolved even though their migration times differ by only ~ 12 s.

The dependences of the product concentrations on dose are given in Figure 3. The concentrations of the dihydroxytoluenes were determined from mass chromatograms recorded at mass 125 and of methylquinone from spectrophotometric recordings at 250 nm. The concentrations of products resulting from •OH attack at the 4 position of *m*-cresol are taken as the sum of those of methylhydroquinone and methylquinone. All of the plots extrapolate to zero at zero dose showing that, as expected, all represent initial products.

Because the cresol concentration in this study is only 5 mM, there is significant and increasing competition of the products with the cresol as the radiolysis progresses so that, as is seen in Figure 3, the yields of products decrease with increasing dose. One is, of course, primarily interested in the initial yields so it is important to establish the initial slopes of these dose dependences. These initial slopes ($d[C_i]_0/dD$) can be determined

TABLE 1: Yields of •OH Adducts^a

product	position of •OH addition ^f	position of OH	position of CH ₃	yield
Phenol ^b				
catechol	2	ortho		1.48×2
resorcinol	3	meta		0.22×2
hydroquinone	4	para		2.14
Toluene ^c				
<i>o</i> -cresol	2		ortho	1.38×2
<i>m</i> -cresol	3		meta	0.68×2
<i>p</i> -cresol	4		para	1.65
<i>p</i> -cresol ^d				
4-methylcatechol	2	ortho	meta	1.55×2
4-methylresorcinol	3	meta	ortho	0.80×2
<i>m</i> -Cresol ^e				
3-methylcatechol	2	ortho	ortho	1.31
methylhydroquinone	4	para	ortho	2.08
5-methylresorcinol	5	meta	meta	0.28
4-methylcatechol	6	ortho	para	1.66
<i>o</i> -Cresol ^f				
2-methylresorcinol	3	meta	ortho	0.67
methylhydroquinone	4	para	meta	1.96
4-methylresorcinol;	5	meta	para	0.69
3-methylcatechol	6	ortho	meta	1.40

^a Initial yields in molecules per 100 eV of absorbed energy at unsubstituted positions relative to OH in the cases of phenol and cresols, relative to methyl in the case of toluene. ^b Reference 5 and 6, total yield 5.54. ^c Reference 7, benzyl alcohol is produced with a yield of 0.07, total yield 5.84. ^d *p*-Hydroxybenzyl alcohol is produced with a yield of 0.55; *p*-dienone is produced with a yield of 0.6 ref 11; total yield 5.85. ^e *m*-Hydroxybenzyl alcohol is produced with a yield ~ 0.01 ; total yield 5.33. ^f *o*-Hydroxybenzyl alcohol is produced with a yield of 0.32. The arguments given in the text suggest that *o*-dienone is produced with a yield ~ 0.4 ; total yield ~ 5.44 .

with considerable accuracy using a relation of the form

$$[C_i]D = d[C_i]_0/dD\{2(\ln(1 + QD)/Q) - D\} \quad (1)$$

where $[C_i]D$ is the concentration of product *i* at dose *D* and

$$Q = k_2/k_1(d[C]/dD)_0/[T] \quad (2)$$

In eq 2, $[C]$ is the total concentration of products. The parameter *Q* provides a measure of the curvature of the plots in the figure. It assumes that the ratios of the rate constants for reaction of •OH with each of the initial products and with the cresols are the same. Given this proviso, *Q* should have a common value for the different products; i.e., all of the products should have similar curvatures. Equation 1 takes into account the above-mentioned competition and also the consumption of product in the secondary reactions. It is applicable during the early stages of radiolysis when tertiary processes are relatively unimportant. Discussion of this equation is given in more detail in Appendix A of ref 11. The initial yields given in Table 1 correspond to the slopes of the tangents to the plots at zero dose indicated by the dashed lines in Figure 3.

B. *p*-Cresol. Because of its symmetry, only 4-methylcatechol and 4-methylresorcinol are expected as the result of addition of •OH at the unsubstituted positions of *p*-cresol. Hydroxylation of the methyl group should also produce 4-hydroxybenzyl alcohol. These products are apparent in the contour plots of the LC and CE data given in Figures 2S and 3S.

However, a fourth initial product, that has a strong absorption at 228 nm (see Figure 4), is manifest at 6.35 min in Figure 2S and at 6.75 min in Figure 3S. In a previous study,⁸ this product has been conclusively identified by its NMR spectrum as 4-hydroxy-4-methyl-2,5-cyclohexadiene-1-one (i.e., *p*-dienone).

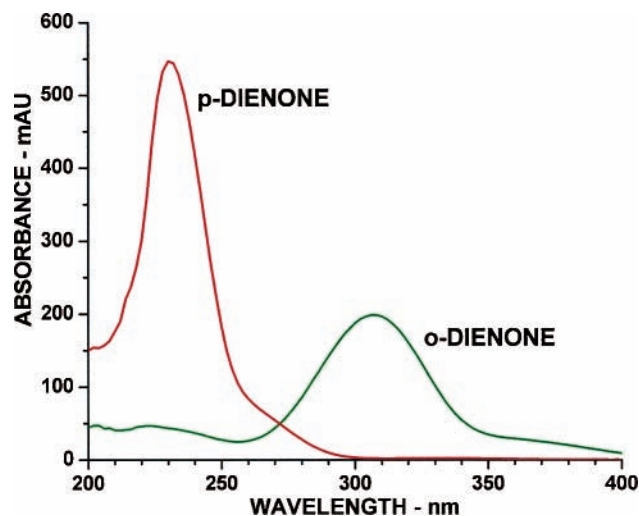


Figure 4. Absorption spectra of *o*- and *p*-dienone normalized for the estimated difference in yields. Note that these spectra have similar low energy sidebands. The extinction coefficient of *p*-dienone at 228 nm has been determined to be $12000 \text{ M}^{-1} \text{ cm}^{-1}$.⁸

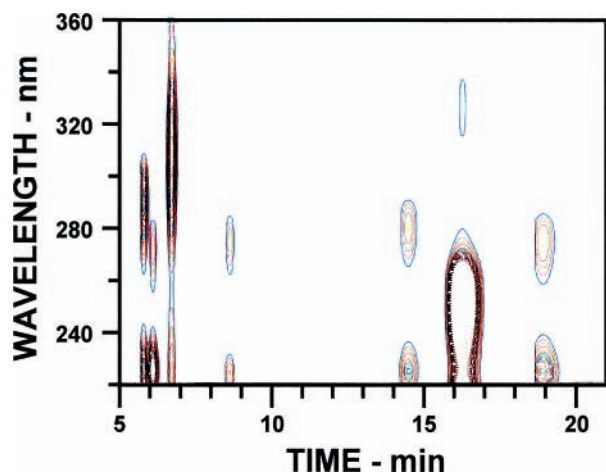


Figure 5. Contour plot of LC data for a 5 mM *o*-cresol solution irradiated to a dose of 2.2 kGy. Contours are at intervals of 4 mAU. Contributions (from left to right) are identified as methylhydroquinone, 5-methylresorcinol, *o*-dienone, 2-hydroxybenzyl alcohol, 4-methylresorcinol, methylquinone, and 3-methylcatechol. See Figure 6S for a complementary contour plot of CE data.

It is produced as the result of $\bullet\text{OH}$ addition to the ring at the methyl position followed by loss of the phenolic proton on oxidation of the intermediate radical.

Electropherograms extracted from the CE data at 228 and 275 nm are given in Figure 4S. The concentration of *p*-dienone was determined from its area in the 228 nm electropherogram and the other products from their areas in the electropherograms extracted at 275 nm. The sensitivity of *p*-dienone was previously determined using a reference sample prepared radiolytically.⁸ The dose dependences of these products, given in Figure 5S, show that all four are initial products that result from oxidation of the radical adducts. The yields of these products, determined from their initial slopes, are given in Table 1.

C. *o*-Cresol. In the case of *o*-cresol, five initial products are expected, but seven are apparent in the contour plot of LC data in Figure 5. Four of these are readily identified (see figure caption) as the dihydroxytoluenes expected to result from addition of $\bullet\text{OH}$ at the unsubstituted positions of *o*-cresol. In addition, 2-hydroxybenzyl alcohol is produced by hydroxylation of the methyl group, and as in the case of *m*-cresol,

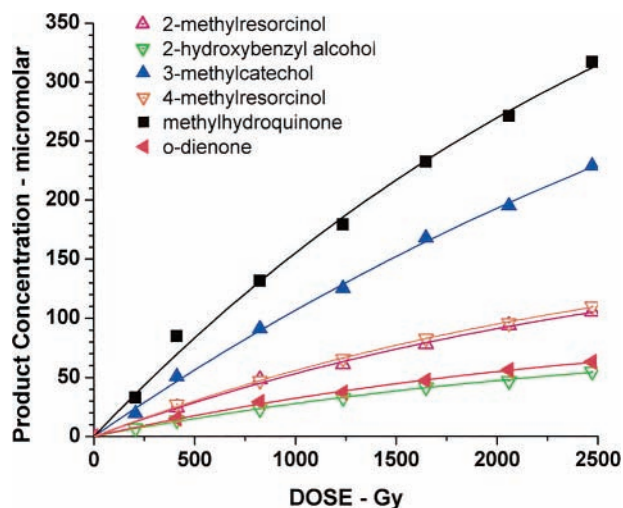
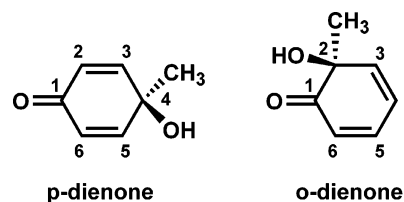


Figure 6. Dose dependence of the products produced in the irradiation of N_2O saturated solutions 5 mM in *o*-cresol. Black squares represent the sum of methylhydroquinone and methylquinone. Data are fitted by eq 1 given in the text.

methylquinone results from chemical oxidation of methylhydroquinone.

A seventh product has a broad moderately intense absorption at 305 nm appears as the third peak in the contour plot of the LC data given in Figure 5 and as the first peak of the plot of the CE data given in Figure 6S. It has the spectrum given in Figure 4. Essentially identical spectra were observed in the acidic environment of the LC studies and the basic environment of the CE studies. This similarity indicates this product to be neutral. It has a dose dependence (see Figure 6) that shows it to be an initial product. Because products have been assigned to all the other possible sites for $\bullet\text{OH}$ attack on *o*-cresol, this contribution must be attributed to a product that results from $\bullet\text{OH}$ addition to the ring at its methyl position. The similarity of the conjugation in the intermediate methylhydroxycyclohexadienyl radicals produced in the cases of *o*- and *p*-cresol suggests that this product has a structure closely related to the *p*-dienone produced in the case of *p*-cresol, i.e., that it is the *o*-dienone 2-hydroxy-2-methyl-3,5-cyclohexadiene-1-one.



As discussed below, the chromatographic, electrophoretic, spectrophotometric, and mass spectrometric properties of this seventh product show it to be this *o*-dienone. Unfortunately, it is considerably less stable than its *para* isomer so that we have not, as yet, been able to isolate it in sufficient quantity to determine its NMR spectrum. These two dienones differ only in the details of conjugation with the carbonyl group terminal rather than central to the diene system.

Electropherograms extracted from CE data are displayed in Figure 7S. It is seen in this figure that *o*-dienone absorbs as strongly at 305 nm as does 4-methylresorcinol at 275 nm even though its yield is estimated to be only half as great. This comparison indicates that its extinction coefficient is $\sim 4000 \text{ M}^{-1} \text{ cm}^{-1}$ at 305 nm. In agreement, the comparison of the spectra in Figure 4 shows its extinction coefficient to be about

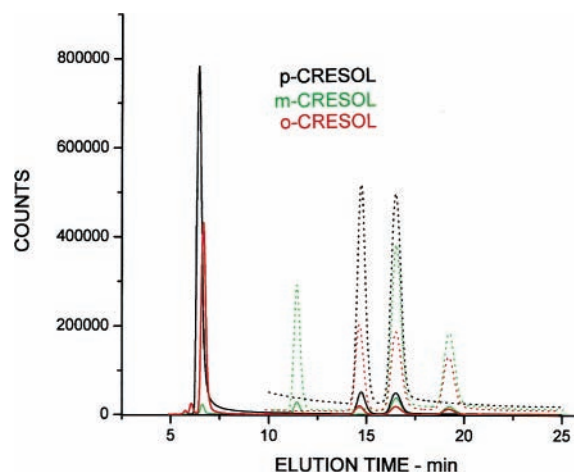


Figure 7. LC chromatograms recorded mass spectrometrically at mass 125 using ES ionization. Dashed chromatograms are displayed at 10-fold greater sensitivity. The two most intense peaks at ~ 6.8 min are attributed to *p*- and *o*-dienone and the other less intense peaks to dihydroxytoluenes.

one-third of that for *p*-dienone at 228 nm, indicating that it has a somewhat lower oscillator strength than does its *para* isomer.

The dose dependences of the various products are given in Figure 6, and their yields, determined from the initial slopes, are given in Table 1. It is seen in this figure that 2- and 4-methylresorcinol are produced with very similar yields. It is particularly noted that the dose dependence for the formation of the *o*-dienone clearly indicates it to be an initial product.

IV. Results: Mass Spectrometric Studies

A. General. Mass spectrometric studies were carried out primarily to provide mass data on the products resulting from •OH addition at the methyl positions of *o*- and *p*-cresol. They also provide quantitative data on the other products in accord with the data obtained spectrophotometrically.

Electrospray recordings of reference samples of the dihydroxytoluenes (mass 124) showed their principal positive ions to be, as expected for ES, at mass 125. Except for methylhydroquinone, all have mass 125 sensitivities of the same magnitude. Hydroxybenzyl alcohols were observed only at mass 107 and do not contribute to mass 125 chromatograms. At high concentrations, methylquinone (mass 122) exhibits an ES signal at mass 123 and a less intense signal at mass 125. However, at the low concentrations present in the irradiated samples it is observed at mass 125, indicating that it is partially reduced to methylhydroquinone in the ion source.

Chemical ionization recordings differ considerably in that, while the methylresorcinols are observed at mass 125, mass 123 is dominant in the CI spectra of the methylcatechols. This difference results from the *ortho*-effect that arises in CI because of conjugation between *ortho* substituents.¹² Because of this *ortho*-effect, methylhydroquinone exhibits a signal at mass 123 in addition to that at mass 125. The CI pattern observed for methylquinone is essentially identical to that for methylhydroquinone, indicating, as suggested above, that methylquinone is reduced to methylhydroquinone in the ion source.

B. Electrospray Studies. Chromatograms recorded at mass 125 for irradiated samples of each of the cresols are given in Figure 7. Peaks of the dihydroxytoluenes and methylquinone are observed at the elution times expected from corresponding spectrophotometric recordings. These mass chromatograms are considerably simpler than those obtained spectrophotometrically

in that secondary products do not contribute at mass 125. Also, while the hydroxybenzyl alcohols exhibit relatively intense mass 107 peaks, they do not contribute in Figure 7.

The mass 125 chromatogram for *m*-cresol exhibits three peaks readily attributable to 5-methylresorcinol, 4-methylcatechol, and 3-methylcatechol at, respectively, 11.5, 16.4, and 19.0 min. The peak at 16.4 min in Figure 7 is, however, also due to an unresolved contribution of methylquinone, but the sensitivity of the latter is relatively low. Methylhydroquinone is observed in complementary spectrophotometric recordings but has only low intensity in this mass recording. The small peak at 6.4 min is attributed to *p*-dienone produced as the result of a $\sim 2\%$ impurity of *p*-cresol. It appears because of the relatively high sensitivity of *p*-dienone in mass recordings. A peak, attributable to 2-hydroxybenzyl alcohol, is observed at 5.8 min in chromatograms recorded at mass 107. From its intensity, its yield is estimated to be only ~ 0.01 , so this product is not apparent in the spectrophotometric studies.

The ES chromatogram of the products from *p*-cresol in Figure 7 exhibits three peaks that have significant intensity. The peaks at 14.7 and 16.4 min represent contributions of 4-methylresorcinol and 4-methylcatechol. The ES sensitivity of the resorcinol is approximately twice that of the catechol so that they have similar peak intensities. 4-Hydroxybenzyl alcohol is observed at 5.4 min in chromatograms recorded at mass 107 but does not contribute in Figure 7. The intense peak at 6.4 min is readily identified as *p*-dienone by its typical 228 nm absorption observed in related contour plots (see Figures 2S and 3S). In the ES recordings it has an order of magnitude higher intensity than the dihydroxytoluenes that are, however, produced in higher yield.

The mass 125 chromatogram for *o*-cresol in Figure 7 exhibits six peaks that have significant intensity. Of these, four correspond to the contributions from products that result from •OH addition at its unsubstituted positions. As in the case of *m*-cresol, methylquinone is also observed as the result of oxidation of methylhydroquinone. Of particular importance is the sixth and most intense peak at 6.8 min that is identifiable from its absorption spectrum as the *o*-dienone. We particularly note that its intensity is 55% of that of *p*-dienone recorded in a parallel experiment and an order of magnitude higher than the intensities of the other products that are presumably produced in greater yield. With the assumption that the ES sensitivities of the dienones are similar, the yield of the *o*-dienone is estimated to be 0.4. 2-Hydroxybenzyl alcohol is also observed at 5.4 min in chromatograms recorded at mass 107 but does not contribute in Figure 7.

The electrospray mass patterns for the dienones are displayed in Figure 8. These patterns have their principal intensities at mass 125 with small contributions at mass 107 that result from loss of water. Mass 123 is absent in the ES pattern of *p*-dienone and of only very low intensity in that for *o*-dienone. In both cases, the ions observed at mass 126 are entirely attributable to the $\sim 7\%$ natural abundance of ¹³C, i.e., C₇H₈O₂⁺ is the principal ion observed with ES ionization.

C. Chemical Ionization Studies. The CI chromatograms recorded for *o*-cresol at mass 123 and 125 using the chemical ionization source are given in Figure 8S. Peaks are identified as in Figure 7. One notes that the CI intensities of the *o*-dienone peak at masses 123 and 125 are considerably less than that in the ES recording at mass 125 and are comparable to those of 4-methylresorcinol and 3-methylcatechol. It is seen that 3-methylcatechol contributes only to the chromatogram recorded at mass 123.

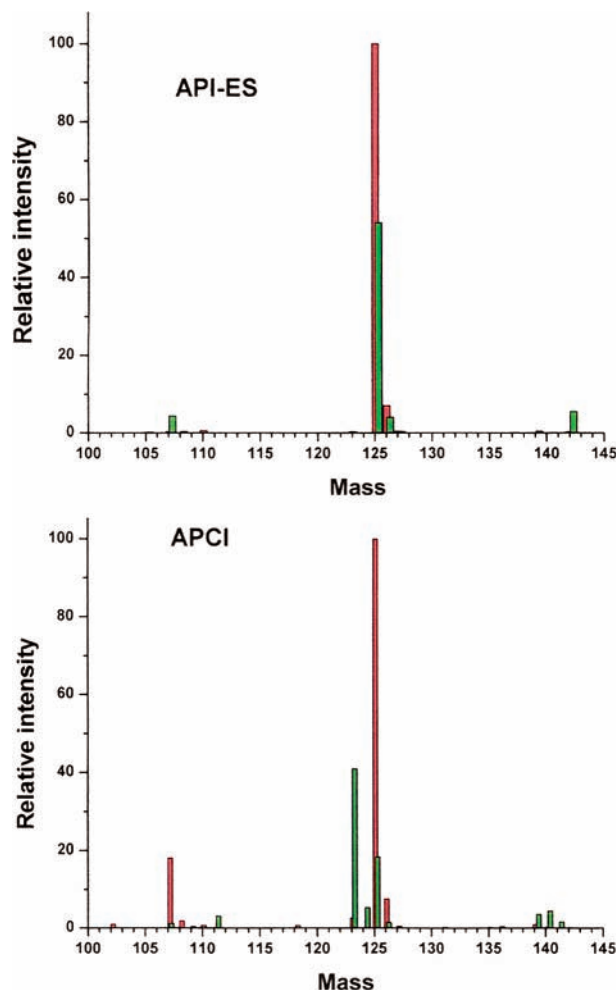


Figure 8. Mass patterns for *p*-dienone (red) and *o*-dienone (green) recorded with electrospray and chemical ionization sources. Patterns for *o*-dienone are normalized by a factor of 1.82 representing the estimated ratio of their yields (0.55).

The mass pattern displayed for the *o*-dienone in Figure 8 shows that *p*-dienone is similar to that observed in ES with only small additional contributions at masses 107 and 123. However, the CI pattern observed for *o*-dienone is much more complex with mass 123 being the most abundant. This difference is a manifestation of the *ortho*-effect, making it clear that this product has an *ortho* configuration. After correction of the mass 124 intensity for its ^{13}C isotopic component, there is a residual intensity that is $\sim 8\%$ of that of mass 123, i.e., so that $\text{C}_7\text{H}_6\text{O}_2^+$ and $\text{C}_7\text{H}_7\text{O}_2^+$ are both produced as fragments in CI. The net intensities of the $\text{C}_7\text{H}_6\text{O}_2^+$, $\text{C}_7\text{H}_7\text{O}_2^+$, and $\text{C}_7\text{H}_8\text{O}_2^+$ ions are in the ratio 100:8:45 showing an *ortho*-effect that is, however, somewhat less pronounced than in the case of the methylcat-echols.

V. Discussion

A. Yields. The initial yields have been summarized in Table 1. For reference, the yields of the hydroxylated products produced from phenol and toluene have been included.

It has previously been shown that the yield for reaction of $\bullet\text{OH}$ radicals with a solute is somewhat dependent the solute concentration.¹³ For solutes that react at diffusion-controlled rates, a yield of 5.9 is estimated from eq 10 in ref 13 for N_2O -saturated solutions at a solute concentration of 5 mM. A yield of 5.85 has been reported for phenol production for a solution 3 mM in benzene⁶ in agreement with that expected at that

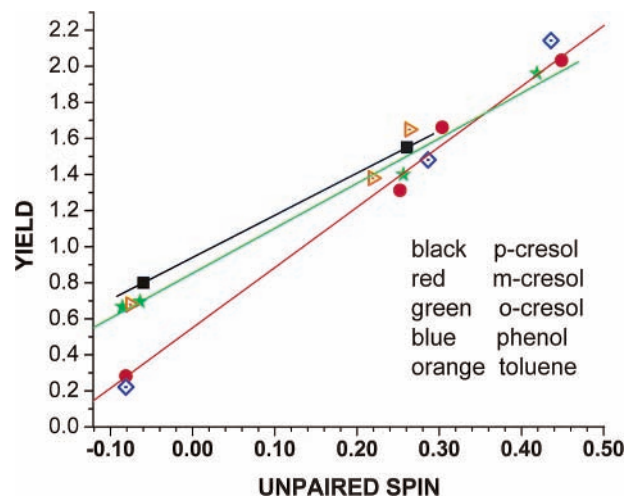


Figure 9. Correlation of the radiation chemical yields with the spin population on the position of addition in the corresponding methylphenoxyl radicals: *p*-cresol (black), *m*-cresol (red), *o*-cresol (green), phenol (open blue diamonds), and benzyl radical (open magenta triangles).

concentration. In the case of toluene, the total yield of products for a solution saturated with toluene (6 mM) is 5.7, only slightly lower than that expected, indicating that $\bullet\text{OH}$ addition at its methyl position is only of minor importance.

The question now arises as to the possible importance of addition to the ring at the hydroxylated positions of phenolics. Such addition would be expected to produce the corresponding phenoxyl radical on loss of water. We note that at solute concentrations of 5 mM the total yields of products observed from the cresols are 5.85, 5.33, and 5.44. These yields indicate that up to $\sim 10\%$ of the $\bullet\text{OH}$ radicals can lead to the reformation of the cresol as the result of reduction of the phenoxyl radicals initially formed or their reaction to give other products. In the case of phenol, time-resolved Raman experiments indicate that $\sim 10\%$ of OH radicals add at the OH position and rapidly eliminate water to give phenoxyl radicals as the initial intermediate.¹⁴

Because $\bullet\text{OH}$ addition to aromatics is essentially diffusion-controlled, the site of addition is determined by the competitions that occur within the reaction complex. Since $\bullet\text{OH}$ is a strong electrophile, it seeks out the more negative sites. As a result, the product distribution observed in these experiments provides a measure of the negative charge distribution in the cresols. We note in Table 1 that the yields for addition to the *meta* position of *m*-cresol are only slightly greater than for addition to the *meta* positions of phenol, indicating that in *m*-cresol the methyl substituent has only a minor effect on the charge distribution. However, the yields for addition at the *meta* positions of *o*- and *p*-cresol are 3-fold greater, showing that methyl substitution at a site *ortho* or *para* to an OH substituent has a substantial effect on the charge distribution in those cresols.

B. Correlation of the Chemical Yields with ESR Hyperfine Data. It is of interest, as is done in Figure 9, to compare the yields in Table 1 with the unpaired spin distributions in the corresponding methylphenoxyl radicals given in Table 2 indicated by ESR data.^{15,16} The similarity of the relations between unpaired spin distribution and charge for phenol and *m*-cresol indicate, as commented on above, that methyl substitution at a *meta* position has little effect on the charge distribution. The fact that the analogous relations in the cases of *o*- and *p*-cresol are similar indicates that methyl substitution has similar effects on the electronic structures of *o*- and *p*-cresol and their corresponding phenoxyl radicals.

TABLE 2: Unpaired Spin Populations^a

radical position ^b	2	3	4	5	6	total
phenoxy	0.29	-0.08	0.44	-0.08	0.29	0.86
benzyl	0.23	-0.08	0.27	-0.08	0.23	0.57
<i>o</i> -methylphenoxy	(0.26)	-0.09	0.43	-0.07	0.26	0.79
<i>m</i> -methylphenoxy	0.26	(-0.05)	0.46	-0.08	0.31	0.90
<i>p</i> -methylphenoxy	0.27	-0.06	(0.43)	-0.06	0.27	0.85

^a Unpaired spin populations at the carbon positions indicated by the ESR hyperfine constants using McConnell coefficients of 23.04 G for the ring protons and of 29.3 G for the protons on the methyl substituents (see ref 15). The latter values are given in parentheses. The proton hyperfine constants (in Gauss) of the ring protons are 6.1 ($\times 2$) and -1.4 ($\times 2$) for *p*-methylphenoxy radical; 10.5, 7.1, 5.9 and -1.9 for *m*-methylphenoxy radical; 9.8, 6.0, -1.5, and -2.0 for *o*-methylphenoxy radical; 10, 6(2), and -2.0(2) for phenoxy radical; and 6.0, 5.0 ($\times 2$), -2.0 ($\times 2$) for benzyl radical (ref 16). The methyl protons have, respectively, values of 7.6, -9.6, and 12.6 G. The methylene protons in benzyl radical have a hfc value of 15 G. ^b Relative to position of OH.

Benzyl radical has an electronic structure similar to phenoxy radical with, however, only 57% of its unpaired spin on the ring. It is noted in Figure 9 that, despite this difference, the correlation of the yields of the cresols produced on addition of •OH to toluene is very similar to that observed for addition of •OH to *o*- and *p*-cresol.

The hyperfine constants of the methyl protons in the methylphenoxy radicals show that there is substantial excess spin on the ring at the methylated positions of *o*- and *p*-methylphenoxy radicals. Assuming that the correlation of the spin and charge distributions given above is applicable, these hyperfine data indicate that there should be a negative charge at those positions in *o*- and *p*-cresol. As a result, •OH is expected to add at the methyl positions of *o*- and *p*-cresol. In the case of *p*-cresol, this expectation is borne out by the finding that *p*-dienone is produced in significant yield. The formation of *o*-dienone from *o*-cresol observed in the present study similarly manifests a high negative charge at its methylated position. The negative spin population at the methyl position of *m*-methylphenoxy radical indicates the charge at the methyl position of *m*-cresol is likely positive so one does not expect attack at that position to be appreciable. In any event, the conjugation in *m*-cresol is such that •OH addition at its methyl position cannot lead to a dienone like product.

C. The Ipsso Adducts. In making the assignment of the 305 nm absorption given in Figure 4 to *o*-dienone, the very large shift from the 228 maximum observed for *p*-dienone was initially of considerable concern. First, we note that its shape is similar to that of *p*-dienone with a similar low energy sideband. The observed shift is effectively explained by application of the Woodward–Fisher rules¹⁷ that describe the dependence of UV absorption spectra on structure. Those rules predict maxima for *p*- and *o*-dienone at, respectively, 230 and 305 nm. The observed maxima are, thus, in complete accord with the wavelengths predicted by the Woodward–Fisher rules. The 77 nm red shift observed experimentally arises from the conjugation between the *ortho* substituents in the *o*-dienone in much the same way as does the *ortho*-effect in the mass spectrometric studies. The absorption spectra, therefore, provide additional substantiation of the assignment of the ~6.6 min peak in Figure 5 to the *o*-dienone.

As indicated in a preceding section, the NMR spectrum of the product resulting from addition of •OH to *p*-cresol at its methyl substituted position conclusively identifies it as *p*-dienone. Its various properties have been described previously in considerable detail.¹¹ The mass patterns given in Figure 8

show that in ES this dienone is protonated and observed, as expected, at mass 125 with a small contribution at mass 107 and essentially no contribution at mass 123. Mass 125 is also dominant in the CI recording with a significant contribution at mass 107 but only a weak signal at mass 123.

In the ES chromatogram given in Figure 7, the intensity of the mass 125 peak of *p*-dienone is seen to be an order-of-magnitude greater than that of the other products that are, however, produced in yields greater by more than a factor of 3.¹¹ The relatively high intensity of this signal indicates that the efficiency for protonation of *p*-dienone is more than a factor of 30 greater than that of its dihydroxytoluene isomers.

Comparison of the various properties of the product from *o*-cresol observed at ~6.6 min in Figure 5, at 6.57 min in Figure 6S and at 6.8 min in Figure 7 shows that it can be identified as the *o*-dienone. As in the case of its *para* isomer, it is produced as the result of loss of the phenolic proton on oxidation of the initial •OH adduct.

First, we note in Figure 7 that in the ES analyses the two intense peaks at ~6.8 min have almost identical retention times and intensities considerably greater than those of the other products. In contrast, their relative intensities observed in the CI experiments are considerably less than those observed in the ES studies. The CI pattern given in Figure 8 has appreciable contributions at masses 123, 124, and 125 as the result of the *ortho*-effect produced by a strong coupling between the two substituents. It is clear from this that the 6.8 min peak in Figure 7 represents a product with an *ortho* configuration. However, in this case the coupling differs from that of the methylcatechols in that while mass 125 has very little intensity in the CI spectrum of 3-methylcatechol it has a substantial intensity in the case of *o*-dienone. This difference indicates that the coupling responsible for the *ortho*-effect is considerably modified when the two substituents are on the same carbon.

D. Concerted Effects. In Table 1, the dominant *ortho*–*para* directing effect of an OH substituent is demonstrated by the high yields for addition at the positions *para* (1.96–2.03) and *ortho* (1.31–1.66) to the OH substituent and the considerably lower yields for addition at the *meta* positions (0.28–0.80). Because the total yield for reaction at the unsubstituted positions of phenol and each of the cresols is different, the competitions that occur within a particular reaction complex are best considered in terms of the ratios of the observed yields for a specific solute. The additional effect of methyl substitution in promoting addition at positions *ortho* to it seen in the ratio of 0.52 observed for addition at the 3 and 2 positions of *p*-cresol and 0.48 at the 6 and 3 positions of *o*-cresol. These ratios compare with the considerably lower value (0.15) observed in the case of phenol. In these cases, the methyl group substantially increases the relative frequency for •OH attack at the position adjacent to it. In the case of *m*-cresol, a ratio of 0.63 is observed for the yields of addition at the 2 and 4 positions that are *ortho* and *para* to OH and also *ortho* to the methyl group. This ratio compares with the ratio of 0.69 observed for addition to the *ortho* and *para* positions of phenol, showing that the effects of the methyl substituent at the *meta* position largely cancel. In the case of *o*-cresol, the yields for addition at the 3 and 5 positions that are *meta* to the OH substituent are similarly affected by methyl groups at the *ortho* and *para* sites but are a factor of ~3 greater than for phenol. Apparently, the presence of the methyl group adjacent to the site of addition in *o*- and *p*-cresol breaks up the conjugation in the cresol sufficiently so as to promote addition at positions *meta* to OH substituents. It is also possible that in the cases of phenol and *m*-cresol the

initial hydroxycyclohexadienyl radicals produced by addition at the *meta* position are less readily oxidized than the other adducts. If this proves to be the case, then one must conclude that the methyl substituent has a significant effect on the oxidation potential.

One would, of course, like to break down the overall effects into a set of contributions more generally applicable. The yields in Table 1 are correlated reasonably well if one takes contributions of 1.35, 0.50, and 1.80 for the sites *ortho*, *meta*, and *para* to the OH substituent and 0.20 for methyl substitution at those sites. These values give yields ~90% of those observed in the case of phenol, about as expected if one takes into account the lower number of reactive sites in the cresols. The principal exception is the low yield (0.28) observed for •OH reaction at the position *meta* to both substituents in *m*-cresol where the values given above indicate the yield should be 0.70. It is, as yet, not clear whether this difference is due to an experimental difficulty in oxidizing the initial radical or more likely, as suggested above, represents a fundamental difference in the effect of the substituents on the charge distribution in *m*-cresol as compared to its isomers.

VI. Summary

The concerted effects of substitution in controlling the reaction site are qualitatively obvious from the above comparisons and generalizations. It is very clear that in the case of the cresols the hydroxyl and methyl substituents act in concert although the effect of OH is dominant. It is found that methyl substitution has only a minor effect on the position of OH addition to *m*-cresol but a substantial effect in the cases of *o*- and *p*-cresol. In the latter cases, the methyl substituent is found to have similar effects on the charge distributions in *o*- and *p*-cresol and on the unpaired spin distributions in the corresponding methylphenoxyl radicals. The observation of *m*- and *p*-dienone as initial products is of extreme importance in demonstrating that •OH addition can occur at the *ipso* positions of alkylated aromatics. In most other cases, stable products do not result from the radicals produced by •OH addition at alkylated positions so that such addition is not readily detected. The relatively high efficiency for proton transfer to *o*- and

p-dienone observed in the electrospray experiments shows that they have significantly high proton affinities.

Acknowledgment. The work described here was supported by the Office of Basic Energy Sciences of the U.S. Department of Energy (R.H.S.) and by UNAM (Grant PAPIIT-100303) and the National Council of Science and Technology of Mexico (Grant CONACYT- 36317E) (G.A.). This is contribution NDRL-4614 from the Notre Dame Radiation Laboratory. The authors wish to thank Dr. William Boggess of the Notre Dame Department of Chemistry and Biochemistry for discussions on the importance of the *ortho*-effect in these studies.

Supporting Information Available: Additional figures. This material is available free of charge via the Internet at <http://pubs.acs.org>.

References and Notes

- (1) Buxton, G. V.; Greenstock, C. L.; Helman, W. P.; Ross, A. B. *J. Phys. Chem. Ref. Data* **1988**, *17*, 513.
- (2) Raghavan, N. V.; Steenken, S. *J. Am. Chem. Soc.* **1980**, *102*, 3495.
- (3) Bhatia, K.; Schuler, R. H. *J. Phys. Chem.* **1974**, *78*, 2335.
- (4) Klein, G. W.; Schuler, R. H. *Radiat. Phys. Chem.* **1978**, *11*, 167.
- (5) Ye, M. Ph.D. Dissertation, University of Notre Dame, Notre Dame, Indiana, 1966.
- (6) Albarran, G.; Schuler, R. H. *Radiat. Phys. Chem.* **2002**, *63*, 661.
- (7) Albarran, G.; Bentley, J.; Schuler, R. H. *J. Phys. Chem. A* **2003**, *107*, 7770.
- (8) Schuler, R. H.; Albarran, G.; Zajicek, J.; George, M. V.; Fessenden, R. W.; Carmichael, I. *J. Phys. Chem. A* **2002**, *106*, 12178.
- (9) The Gray (Gy) is the SI unit for energy deposition in radiation chemical experiments: 1 Gy = 1 J/kg = 100 rads = 6.24×10^{-15} eV/g. Radiation chemical yields are given as G-values in units of molecules per 100 eV of absorbed energy.
- (10) *ORIGIN*; Microcal Software Inc., Northhampton, MA, 1991.
- (11) Albarran, G.; Schuler, R. H. *Radiat. Phys. Chem.* **2003**, *67*, 279.
- (12) See, for example: Smith, R. M. *Understanding Mass Spectra: Second Edition*; Wiley-Interscience: New York, 2004; pp 251–254.
- (13) Schuler, R. H.; Hartzell, A. L.; Behar, B. *J. Phys. Chem.* **1981**, *85*, 192.
- (14) Tripathi, G. N. R.; Su, Y. *J. Phys. Chem. A* **2004**, *108*, 3478.
- (15) Fessenden, R. W.; Schuler, R. H. *J. Chem. Phys.* **1963**, *39*, 2147.
- (16) *Landolt-Bornstein: Numerical Data and Functional Relationships in Science and Technology, New Series II*; Madelung, O., Ed.; Springer-Verlag: Berlin, 1988; Vol. 17e.
- (17) See: Silverstein, R. M.; Bassler, G. C.; Morrill, T. C. *Spectrometric Identification of Organic Compounds*, 3rd ed.; John Wiley & Sons: New York, 1974; Chapter 5.